Gold Surface Functionalization and Patterning for Specific Immobilization of Olfactory Receptors Carried by Nanosomes

ARTICLE *in* ANALYTICAL CHEMISTRY · MAY 2007

Impact Factor: 5.64 · DOI: 10.1021/ac061774m · Source: PubMed

12 AUTHORS, INCLUDING:

David Caballero
IBEC Institute for Bioengineering of Catalonia
26 PUBLICATIONS **199** CITATIONS
SEE PROFILE

Nicole Jaffrezic-Renault
Claude Bernard University Lyon 1
676 PUBLICATIONS **9,407** CITATIONS
SEE PROFILE

Josep Samitier
University of Barcelona
476 PUBLICATIONS **3,859** CITATIONS
SEE PROFILE

Anal. Chem. **2007,** *79,* 3280−3290

Gold Surface Functionalization and Patterning for Specific Immobilization of Olfactory Receptors Carried by Nanosomes

Jasmina Vidic,*,† Mateu Pla-Roca,*,‡ Jeanne Grosclaude,§ Marie-Annick Persuy,† Régine Monnerie,† David Caballero,‡ Abdelhamid Errachid,‡ Yanxia Hou,|| Nicole Jaffrezic-Renault,|| Roland Salesse,† Edith Pajot-Augy,*,† and Josep Samitier‡

Neurobiologie de l'Olfaction et de la Prise Alimentaire, Equipe Récepteurs et Communication Chimique, INRA, Jouy en Josas, France, Institut de Bioenginyeria de Catalunya (IBEC), Universitat de Barcelona, Barcelona, Spain, Unité de Virologie et Immunologie Moléculaires, INRA, Jouy-en-Josas, France, and CNRS, CEGELY, Ecole Centrale de Lyon, Bat. H9, 69134 Ecully Cedex, France

There is substantial interest in engineering solid supports to achieve functional immobilization of membrane receptors both for investigation of their biological function and for the development of novel biosensors. Three simple and practical strategies for immobilization of a human olfactory receptor carried by nanosomes are presented. The basis of the functionalization of solid gold surfaces is a self-assembled monolayer (SAM) containing biotinyl groups. Biotinyl groups are subsequently used to attach neutravidin and then biotinylated monoclonal antibody directed against the receptor to allow its specific grafting. Surface plasmon resonance technique is implemented for real-time monitoring of step-by-step surface functionalization and, in addition, for testing the functional response of immobilized olfactory receptors. We show that OR1740 is functional when immobilized via a tag attached to its C-terminus, but not via its N-terminus. Finally, we demonstrate that gold surfaces can be patterned by the SAMs tested using microcontact printing. AFM images of immobilized nanosomes onto a patterned surface suggest that small nanosomes flatten and fuse into larger vesicles but do not merge into a continuous layer. The whole study emphasizes the outstanding performances of the BAT/PEGAT SAM, which could be useful for developing on-a-chip sensor formats for membrane receptor investigations and use.

The perception and discrimination of thousands of different odorants from the external environment is essential for the survival of individuals and of animal species. Identification and cloning of genes of the family encoding the olfactory receptors by Nobel Prize laureates Buck and Axel[1] opened the way to research on the olfactory system at the molecular level. Olfactory receptors belong to the G-protein coupled receptors (GPCRs) superfamily with a putative 7-transmembrane domains topology. The first common step in mammalian odorant detection is the odorant specific binding to an olfactory receptor, expressed on the ciliae of olfactory sensory neurons, embedded in the olfactory mucosa located in the nasal cavity. The activated olfactory receptor interacts with the $G_{\alpha olf}$ subunit of a heterotrimeric G-protein, which mediates the signaling cascade transmission to the olfactory bulb, where olfactory signals are processed before reaching cortical structures.[2]

Given the prominent properties of animal olfaction (specificity, sensitivity, and low thresholds for odorant detection), it is tempting to harness olfactory receptors to some device to yield an olfactory biosensor. Major challenges for achieving such a biosensor are as follows: (i) sample preparation to maintain receptor activity, (ii) sample immobilization onto a solid surface, and (iii) development of a functional test. Olfactory biosensor elaboration was hindered in the past due to the absence of natural sources providing individual olfactory receptors in sufficient amounts and to the inherent difficulties associated with the expression of olfactory receptors in heterologous cell systems.[3,4] However, we previously demonstrated that functional expression of olfactory receptors can be achieved at the plasma membrane of *Saccharomyces cerevisiae* by optimizing experimental conditions.[5] In order to meet the first requirement for biosensor development, membrane nanosomes with functional olfactory receptors can be prepared starting from this yeast system by cell disruption, fractionation, and sonication of membrane fraction.[6] Another reported possibility, although at a larger scale, is to coat a sensor surface with living cells expressing olfactory receptors.[7,8]

* Corresponding authors. E-mail: jasmina.vidic@jouy.inra.fr. Fax: + 33 1 34 65 22 41. E-mail: edith.pajot@jouy.inra.fr. Fax: + 33 1 34 65 22 41. E-mail: mpla@pcb.ub.es. Fax: +34 93 4037181.

† Equipe Récepteurs et Communication Chimique, INRA.

‡ Universitat de Barcelona.

§ Unité de Virologie et Immunologie Moléculaires, INRA.

|| Ecole Centrale de Lyon.

(1) Buck, L.; Axel, R. *Cell* **1991**, *65*, 175−187.

(2) Firestein, S. *Nature* **2001**, *413*, 211−218.

(3) McClintock, T. S.; Sammeta, N. *Neuroreport* **2003**, *14*, 1547−1552.

(4) Mombaerts, P. *Nat. Rev. Neurosci.* **2004**, *5*, 263−278.

(5) Minic, J.; Persuy, M. A.; Godel, E.; Aioun, J.; Connerton, I.; Salesse, R.; Pajot-Augy, E. *FEBS J.* **2005**, *272*, 524−537.

(6) Vidic, J. M.; Grosclaude, J.; Persuy, M. A.; Aioun, J.; Salesse, R.; Pajot-Augy, E. *Lab Chip* **2006**, *6*, 1026−1032.

(7) Ko, H. J.; Park, T. H. *Biosens. Bioelectron.* **2005**, *20*, 1327−1332.

(8) Liu, Q.; Cai, H.; Xu, Y.; Li, Y.; Li, R.; Wang, P. *Biosens. Bioelectron.* **2006**, *22*, 318−322.

10.1021/ac061774m CCC: $37.00
Published on Web 03/30/2007

Furthermore, we and others developed several functional tests for studying odorant interaction with membrane-bound olfactory receptors. Surface plasmon resonance (SPR) can be applied for indirect study of olfactory receptor−odorant interaction through the monitoring of $G_{\alpha olf}$ protein desorption induced by receptor stimulation by an odorant ligand.[6] Electrochemical impedance spectroscopy (EIS) is predicted to allow the direct monitoring of electrical properties changes of a single olfactory receptor, generated by its conformational change elicited by the binding of the odorant ligand.[9] This was already demonstrated at the millimetric scale.[10,11] Finally, mass changes due to olfactory receptor−odorant complex formation can be successfully probed using quartz crystal microbalance measurements.[7,12,13]

Olfactory receptors OR1740 and ORI7 carried by nanosomes exhibited a fine discrimination between odorant ligands and unrelated odorants in SPR and EIS experiments,[6,11] as previously observed with a bioluminescence reporter in yeast cells[5] or by calcium response in mammalian cells.[14] This strongly supported the fact that full receptor activity is maintained in the nanosomes. Similarly, Sung et al.[12] have shown that nematode olfactory receptor ODR10 expressed in *Escherichia coli* retains its activity in crude membrane fraction tested by quartz crystal microbalance measurements, since it interacted preferentially with its natural ligand diacetyl as previously observed in nematodes,[15] neurons,[16] or HEK293 cells.[17]

Thus, the challenge still to be achieved was to optimize olfactory receptor immobilization procedures. The SPR technique is well suited for evaluating functionalization procedures, since it provides a means for surface-sensitive, in situ measurements in real time. In our previous SPR study for the development of olfactory biosensors, we used commercial BIAcore L1 sensor chips to immobilize olfactory receptors carried by nanosomes.[6] The L1 chip bears a covalently grafted aliphatic motif acting as a hook to catch nanosomes nonspecifically by their lipid bilayer, whatever their receptor content. However, olfactory receptor purification or enrichment in olfactory-rich nanosomes cannot be considered using classical biochemical methods, regarding the low level of receptor expression in plasma membranes. In consequence, the functional performance of the device can only be enhanced by specific functionalization of the sensor chip surface with a specific antibody against the olfactory receptor, to allow in situ selection of those nanosomes bearing the olfactory receptor of interest. Ideally, the immobilization procedure should promote strong links between receptor and the solid gold surface, a controlled deposition density, a uniform receptor orientation, the receptor full accessibility to ligand, and moreover a minimization of nonspecific odorant interaction with the underlayers.

In this paper, we use SPR measurements to compare three types of gold chip functionalization procedures in terms of their efficiency for immobilization of nanosome-bound olfactory receptors and for their functional response.

EXPERIMENTAL SECTION

Biomaterials and Chemicals. Human olfactory receptor OR1740 (ORL520 in Olfactory receptors Data Base, OrDB) was used in this study as a model receptor. It was heterologously expressed with a cmyc tag fused at its N-terminus in the yeast *S. cerevisiae* as described previously.[5] To perform functional tests, yeast cells were also transformed to coexpress the $G_{\alpha olf}$ protein. In some control experiments, rat OR I7 (ORL11 in OrDB)[5] and doubly tagged OR1740, with a cmyc tag fused at its N-terminus and a HA tag at its C-terminus, were used. Nanosomes were obtained as previously reported.[6] In brief, yeast membrane fraction was prepared and sonicated to obtain nanosomes with a uniform diameter of ∼50 nm.

The total protein concentration in the nanosomes was determined using the BCA reagent (Pierce, Brebieres, France) with bovine serum albumin (BSA) as a standard. The monoclonal mouse anti-cmyc and anti-HA antibodies were biotinylated using a DSB-X Biotin Protein Labeling Kit (Molecular Probes, Leiden, The Netherlands). BATs obtained using solid-phase methodology as described before[18] were kindly supplied by Prof. F. Albericio and E. Prats-Alfonso (IRBB, Barcelona, Spain). PEG-terminated alkanethiols (PEGATs) were purchased from ProChimia Surfaces Sp (Sopot, Poland).

1-Ethyl-3-(dimethylamino)propylcarbodiimide hydrochloride (EDC), pentafluorophenol (PFP), *N*,*N*-diisopropylethylamine (DIPEA), aminoethoxyethanol (AEE), and 16-mercaptohexadecanoic acid (MHDA) were purchased from Sigma-Aldrich (Saint Quentin, France), and 1,2-dioleoyl-*sn*-glycero-3-phosphoethanolamine-*N*-(biotinyl) sodium salt (biotinyl-PE) was purchased from Avanti (Alabaster, AL). (+)-Biotinyl-3,6,9-trioxaundecamine (EZ-Link Amine-PEO3-Biotin) and neutravidin were purchased from Pierce.

The odorants octanal (purity 99%), heptanal (purity 95%), and the solvent dimethylsulfoxide (DMSO) (purity ≥99.9%) were purchased from Sigma-Aldrich. Helional was a generous gift from Givaudan-Roure, courtesy of Boris Schilling (CH-Dubendorf). Stock solutions (10^{-1} M) were prepared each day in DMSO, and 10^{-4} M dilutions in water were made extemporaneously, directly from the 10^{-1} M stock solution. Further dilutions were prepared by successive 1/10 dilutions in water.

SPR Experiments. SPR experiments were conducted on a BIAcore 3000 (Pharmacia Biosensor). Gold sensor chips (BIAcore Au sensor chips), were functionalized with self-assembled mono-

(9) Pennetta, C.; Akimov, V.; Alfinito, E.; Reggiani, L.; Gorojankina, T.; Minic, J.; Pajot-Augy, E.; Persuy, M.-A.; Salesse, R.; Casuso, I.; Errachid, A.; Gomila, G.; Ruiz, O.; Samitier, J.; Hou, Y.; Jaffrezic, N.; Ferrari, G.; Fumagalli, L.; Sampietro, M. *Nanotechnol. Life Sci.* **2006**, *4*, 217−240.

(10) Gomila, G.; Casuso, I.; Errachid, A.; Ruiz, O.; Pajot, E.; Minic, J.; Gorojankina, T.; Persuy, M. A.; Aioun, J.; Salesse, R.; Bausells, J.; Villaneuva, G.; Rius, G.; Hou, Y.; Jaffrezic, N.; Pennetta, C.; Alfinito, E.; Akimov, V.; Reggiani, L.; Ferrare, G.; Fumagalli, L.; Sampietro, M.; Samitier, J. *Sens. Actuators, B: Chem.* **2006**, *116*, 66−71.

(11) Hou, Y.; Jaffrezic-Renault, N.; Martelet, C.; Zhang, A.; Minic-Vidic, J.; Gorojankina, T.; Persuy, M. A.; Pajot-Augy, E.; Salesse, R.; Akimov, V.; Reggiani, L.; Pennetta, C.; Alfinito, E.; Ruiz, O.; Gomila, G.; Samitier, J.; Errachid, A. *Biosens. Bioelectron.* **2006**.

(12) Sung, J. H.; Ko, H. J.; Park, T. H. *Biosens. Bioelectron.* **2006**, *21*, 1981−1986.

(13) Rodriguez Segui, S. R.; Pla, M.; Minic, J.; Pajot-Augy, E.; Salesse, R.; Hou, Y.; Jaffrezic-Renault, N.; Mills, C. A.; Samitier, J.; Errachid, A. *Anal. Lett.* **2006**, *39*, 1735−1745.

(14) Levasseur, G.; Persuy, M. A.; Grebert, D.; Remy, J. J.; Salesse, R.; Pajot-Augy, E. *Eur. J. Biochem.* **2003**, *270*, 2905−2912.

(15) Chou, J. H.; Troemel, E. R.; Sengupta, P.; Colbert, H. A.; Tong, L.; Tobin, D. M.; Roayaie, K.; Crump, J. G.; Dwyer, N. D.; Bargmann, C. I. *Cold Spring Harbor Symp. Quant. Biol.* **1996**, *61*, 157−164.

(16) Sengupta, P.; Chou, J. H.; Bargmann, C. I. *Cell* **1996**, *84*, 899−909.

(17) Zhang, Y.; Chou, J. H.; Bradley, J.; Bargmann, C. I.; Zinn, K. *Proc. Natl. Acad. Sci. U.S.A.* **1997**, *94*, 12162−12167.

(18) Prats-Alfonso, E. G.-M. F.; Bayo, N.; Cruz, L. J.; Pla-Roca, M.; Samitier, J.; Errachid, A.; Albericio, F. *Tetrahedon* **2006**, *62*, 6876−6881.

layers (SAM)1−3 as follows. SAM1 was obtained by 72-h incubation of a mixture of BATs (0.01 mM) and PEGATs (0.09 mM) dissolved in ethanol, followed by rinsing several times with absolute ethanol. To produce SAM2, the gold chip was incubated with a solution of MHDA (1 mM) in ethanol during 72 h to obtain an acid-terminated SAM. Afterward, the chip was immersed for 15 min in a mixture of EDC (0.1M), PFP (0.2 M), and DIPEA (0.1 M) in absolute ethanol, in order to activate the acid groups. After rinsing with absolute ethanol, the surface was functionalized with biotinyl groups by immersion in EZ-Link Amino-PEO3-Biotin (10 mM) in ethanol. In order to produce SAM3, the gold sensor surface was immersed in a mixture of MHDA (1 mM) and biotinyl-PE (0.1 mM) in ethanol during 24 h. Next, the surface was rinsed with absolute ethanol.

Nanosomes were diluted in HBS buffer (25 mM HEPES, pH 7.4, containing 150 mM NaCl) before deposition. Nanosomes were run onto sensor chips at a low flow rate (2 μL/min) for 20 min until a stable resonance unit (RU) level was obtained. Protein-free buffer solution was then injected to rinse off noncaptured material and reach deposition equilibrium. Functional tests were performed with odorants at various concentrations in HBS containing 10 μM GTPγS, at a 5 μL/min flow rate. In control experiments, stimulation was carried out using solutions in which the odorant had been replaced by water. The quantitative responses were calculated as the difference to the corresponding controls, so that the solution contained the same DMSO and the same GTPγS concentrations. All measurements were performed at 25 °C. RU levels were compared before and after each injection, to evaluate the amount of material grafted onto the sensor chip.

Immunoblot Analysis. Proteins of the membrane fraction were separated by electrophoresis on 12% SDS−polyacrylamide gels and electrotransferred onto Hybond-C Extra membrane (Amersham Pharmacia Biotech Europe, Orsay, France). The membrane was blocked with 4.5% no-fat dry milk in 150 mM NaCl, 10 mM PO_4, pH 7.4 sodium phosphate buffer saline (PBS). Membranes were incubated overnight at 4 °C with mouse anti-cmyc monoclonal antibody (Roche, Meylan, France), at 1 μg/mL in 4.5% no-fat dry milk in PBS. After washing, membranes were incubated for 1 h at room temperature with anti-mouse IgG conjugated to horseradish peroxidase (1/2000) diluted in the same buffer. Blots were revealed using the enhanced chemiluminescence detection kit from Amersham Pharmacia Biotech Europe.

Immunodetection and Electron Microscopy. For ultrastructural localization of the olfactory receptors in nanosomes, nanosomes carrying cmyc-OR1740 were adsorbed over TEM grids coated with Formvar, permeabilized with saturated meta-periodate water solution for 1 h at room temperature, and washed with water, then with 0.1M HCl (10 min), and again with water. Free aldehydic sites were quenched by incubation with 2% glycine in PBS. Afterward, nonspecific sites were blocked with incubating buffer consisting of 10% normal goat serum and 5% BSA, 0.5% Triton X-100, and 0.5% Tween 20 in PBS for 1 h. After several washes in the incubation buffer, grids were incubated overnight with the anti-cmyc antibody (1/100 dilution) in the incubation buffer in a wet chamber at 4 °C. They were washed in PBS containing 0.1% acetylated BSA (PBS−BSAc, Aurion, Wageningen, Netherlands) and then incubated with 10-nm gold-conjugated goat anti-rabbit F(ab')2 fragments (Aurion) diluted 1/40 in PBS−BSAc for 1.5 h at room temperature. After extensive washes in PBS−BSAc and PBS, the antigen−antibody complex was stabilized with 2.5% glutaraldehyde in PBS. The preparations were then contrasted using Reynolds' lead citrate before observation. Controls for the immunocytochemical reaction were carried out by replacing either the primary or the secondary antibody by the incubation buffer in the reaction sequence. The grids were finally viewed under a JEOL 1010 transmission electron microscope.

Atomic Force Microscopy Characterization. All the samples were characterized using a commercial Dimension 3100 AFM (Veeco Instruments) in air medium at room temperature with a relative humidity of ~30%. The measurements were performed in contact mode, using rectangular silicon AFM tips of 460 μm in length (MikroMasch CSC17/AlBS, a spring constant of 0.15 N/m, a resonance frequency of 12 kHz, a radius of curvature of ~10 nm, aluminum backside coating). A minimal force was applied in order to minimize sample modification. It was checked that no damage to the biological samples occurred by comparing several successive AFM recordings over the same area. AFM images were analyzed with the WSxM software from Nanotec ElectronicaTM.

Microcontact Printing. An elastomeric stamp was fabricated for microcontact printing as described previously[19,20] All gold substrates were made of cleaved mica with a 150-nm-thick gold layer (Molecular Imaging, distributed by ScienTec). First, silicon-based molds were elaborated using deep reactive ion etching. Positive and negative poly(dimethylsiloxane) (PDMS; Sylgard 184, Dow Corning) stamps were then replicated from these molds. Negative stamps contain holes 800 nm deep and with a 2.5-μm diameter, while the positive stamps present round posts of 2.5-μm diameter that protrude 800 nm from the surface.

All inking procedures of the stamp were performed after hydrophilization of PDMS surface with oxygen plasma (Plasma Cleaner, Harrick Plasma) in order to ensure the correct surface coverage by the ink. To produce patterned SAM1 on a gold surface, a positive stamp was inked during 1 min with 4 mM acetonitrile solution of BAT, dried with N_2, and brought into contact with the gold surface. Blocking of the remaining gold surface was achieved by immersion of the sample in 1 mM PEGAT solution in ethanol during 24 h. Patterning SAM2 on gold was based on a described procedure.[18,21] First, gold surfaces were functionalized with MHDA as described for Biacore gold sensor chips. Then, a positive stamp was inked with a 10 mM ethanolic solution of EZ-link Amine-PEO3-Biotin, dried with N_2, and brought into contact with the MHDA acid during 10 min. Finally, the surface was immersed in a 10 mM AEE solution in 100 mM sodium bicarbonate buffer (pH 8.3) for 20 min in order to block the remaining acid-activated groups and rinsed with Milli-Q water and absolute ethanol in order to remove chemical impurities.

Patterning of SAM3 was obtained by inking a negative stamp with a 4 mM ethanol PEGAT solution. After drying, the stamp was placed into contact with the gold surface during 1 min. The patterned surface was immersed within the SAM3 mixture (MHDA/biotinyl-PE) in order to adsorb the biotin-terminated monolayer on the remaining free gold surface.

(19) Hyun, J. Z. Y.; Liebmann-Vinson, A.; Beebe, T. P., Jr.; Chilkoti, A. *Langmuir* **2001**, *17*, 6358−6367.
(20) Xia, Y. W. G. M. *Angew. Chem., Int. Ed. Engl.* **1998**, *37*, 550−575.
(21) Yang, Z.; Belu, A. M.; Liebmann-Vinson, A.; Sugg, H.; Chilkoti, A. *Langmuir* **2000**, *16*, 7482−7492.

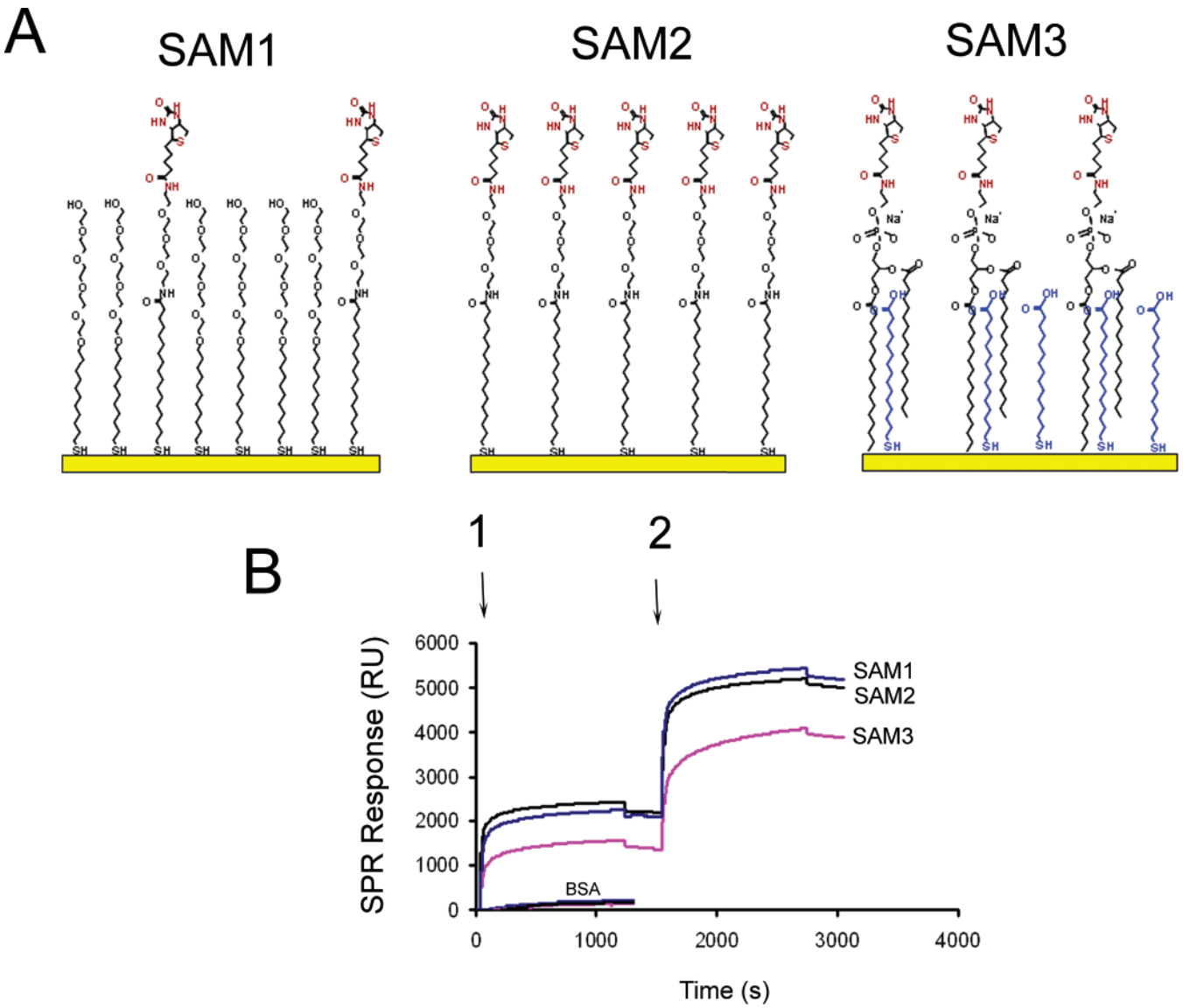

Figure 1. (A) Schematic view of the SAM thiols attached to the gold chip. Biotin groups on top are shown in red. MHDA in SAM3 appears in blue. (B) SPR sensorgrams showing (1) neutravidin (500 nM), and (2) biotinylated anti-cmyc antibody (1 μM) injection on surfaces modified by SAMs and the levels obtained after each equilibrium step. In addition, BSA (1 μM) injection on any SAM is presented at the same scale for purpose of comparison to neutravidin.

RESULTS AND DISCUSSION

Gold Chip Functionalization by Self-Assembled Monolayers. Three types of SAMs carrying biotinyl groups, for convenience named SAM1−3, were studied (Figure 1A). SAM1 was obtained by deposition of a mixture of BATs and PEGATs (ratio 1/9). This mixed SAM allows easy control of the surface binding site density for neutravidin as a function of BAT percentage in the solution used to prepare the surface.[18,22,23] The formation of SAM2 consists first in the deposition of a MHDA and then in its activation by a mixture of EDC/PFP/DIPEA.[19] The EZ-link Amino-PO3-Biotin is subsequently attached onto the surface to allow neutravidin grafting. Finally SAM3 was obtained by deposition of a mixture MHDA/biotinyl-PE (ratio 10/1), providing immobilization of biotinyl groups between self-assembled MHDA molecules.[11,24,25] Again, the ratio between the components in solution determines the final density of biotin anchoring sites at the surface.[25] For all three SAMs, the experimental conditions used to obtain the final surface concentrations of biotinyl groups are those previously reported as optimal to yield high streptavidin binding.[18,19,25]

SPR experiments were performed to compare the efficiency of the three SAMs regarding neutravidin (500 nM) and subsequent biotinylated anti-cmyc antibody (1 μM) immobilization. There is almost no significant difference between SAM1 and SAM2 in terms

(22) Jung, L. S. N. K. E.; Campbell, C. T.; Stayton, P. S.; Yee, S. S.; Pérez-Luna, V.; López, G. P. *Sens. Actuators, B: Chem.* **1999**, *54*, 137−144.
(23) Nelson, K. E. G. L.; Jung, L. S.; Boeckl, M. S.; Naeemi, E.; Golledge, S. L.; Sasaki, T.; Castner, D. G.; Campbell, C. T.; Stayton, P. S. *Langmuir* **2001**, *17*, 2807−2816.
(24) Minic, J.; Grosclaude, J.; Aioun, J.; Persuy, M. A.; Gorojankina, T.; Salesse, R.; Pajot-Augy, E.; Hou, Y.; Helali, S.; Jaffrezic-Renault, N.; Bessueille, F.; Errachid, A.; Gomila, G.; Ruiz, O.; Samitier, J. *Biochim. Biophys. Acta* **2005**, *1724*, 324−332.
(25) Hou, Y.; Helali, S.; Zhang, A.; Jaffrezic-Renault, N.; Martelet, C.; Minic, J.; Gorojankina, T.; Persuy, M. A.; Pajot-Augy, E.; Salesse, R.; Bessueille, F.; Samitier, J.; Errachid, A.; Akimov, V.; Reggiani, L.; Pennetta, C.; Alfinito, E. *Biosens. Bioelectron.* **2006**, *21*, 1393−1402.

Table 1. SPR Evaluation of Specific Binding of Neutravidin, Biotinylated Anti-cmyc Antibody (BiotAb), and cmyc-OR1740 Carried by Nanosomes onto a Gold Surface Functionalized with SAM1, SAM2, or SAM3[a]

surface	neutravidin (RU)	Biot-Ab (RU)	ratio BiotAb neutravidin		OR1740 receptor capture (RU)		ratio OR1740 receptor/Ab capture	
			− BSA	+ BSA	− BSA	+ BSA	− BSA	+ BSA
SAM1	2224 ± 98	3414 ± 181	1.54	1.50	585 ± 43	574 ± 32	0.17	0.19
SAM2	2373 ± 154	2672 ± 212	1.13	1.12	650 ± 95	575 ± 24	0.24	0.22
SAM3	**1073 ± 180**	**1791 ± 380**	1.67	0.89	**4076 ± 514**	**4194 ± 210**	2.27	2.74

[a] Specific binding is evaluated by differential measurement in the absence (−) and the presence (+) of BSA, to estimate the influence of protein adsorption onto the biostructured surfaces. Results are an average of 4 independent measurements; mean ± SD. Contrasting values as compared to other SAMs are highlighted in boldface type.

of efficiency for neutravidin and biotinylated antibody immobilization (Figure 1B). In contrast, we observe the lowest immobilization level of both neutravidin and biotinylated antibody on SAM3 (Table 1, columns 1 and 2). This can arise from either a too small or a too high surface density for biotinyl groups in SAM3, as compared to SAM1 or SAM2. Indeed, previous investigations of mixed SAMs have shown that the amount of bound streptavidin reaches a maximum in a relatively narrow range of surface concentrations of biotinyl groups (10−30% of biotin in mixed SAMs).[22,23,26,27] Since biotin binding pockets are located in pairs at opposite sites of the neutravidin molecule, it can be assumed that a fraction of the neutravidin can attach to the surface through a single biotin−neutravidin bond, whereas another fraction can bind through two biotin−neutravidin bonds.[23] The stability of a SAM is improved when neutravidin binds to two biotin groups. However, at high concentrations of BAT, the level of immobilized neutravidin usually decreases. It has been hypothesized that high BAT concentrations induce a densely packed layer of biotin on the surface, which can sterically inhibit biotin interaction with one of the neutravidin binding pockets.[28] High surface concentration of BATs at the gold surface can also decrease the concentration of biotin head groups available for neutravidin binding, due to the loss of upright orientation of the BAT in such BAT-rich layers.[23]

To assess the specificity of neutravidin grafting on SAMs, BSA immobilization was probed. BSA is a slightly larger protein than neutravidin (60 vs 52 kDa). Applied at a concentration twice that of neutravidin (1 μM vs 500 nM), BSA induced a much lower SPR response shift than neutravidin (<150 RU for BSA, compared with several thousands RU observed for neutravidin, all SAMs), thus demonstrating neutravidin grafting specificity.

Next, we probed whether surface pretreatment with BSA-modified immobilization of neutravidin or biotinylated cmyc-antibody. As shown in Table 1 (column 3), BSA presaturation has a significant effect only on SAM3, while SAM1 and SAM2 displayed no change in corresponding binding efficiencies.

In order to quantify the efficiency of biotinylated anti-cmyc antibody immobilization, we calculated the ratios of SPR responses observed for antibody relative to neutravidin grafting on all three SAMs. If we assume a one-to-one antibody/neutravidin binding ratio and that SPR response is proportional to the bound mass amount, the stoichiometric ratio should have a value of ∼2, considering their respective molecular mass (120 vs 60 kDa). Strikingly, a ratio of only 1.5, 1.1, and 1.7 was obtained for SAM1, SAM2, and SAM3, respectively (Table 1, column 3). This suggests that probably not all biotin binding sites in immobilized neutravidin molecules are accessible for biotinylated antibody binding.

Overall, these last two findings suggest that neutravidin binding capacity of SAM1 and SAM2 are determined by the number of available biotinyl groups, while the binding capacity of SAM3 appears to arise from both specific and nonspecific protein immobilization. The shape and the level of SPR responses observed for neutravidin and biotinylated anti-cmyc antibody grafting give evidence of the efficiency of SAM1 and SAM2. In contrast, the lower level reached for SAM3 indicates that some improvement could still be achieved.

Nanosomes Characterization. Since olfactory receptors have seven membrane-spanning domains, they require an extremely hydrophobic environment (lipids or detergents) to maintain their native conformation and function. To overcome the problems of losing or altering receptor function that can arise during their purification in a detergent and reconstitution in artificial membranes, we recently proposed a strategy of nanosomes sample preparation.[6] Being produced from yeast cells in which receptors have been expressed, nanosomes ensure that olfactory receptors are maintained at all times in the natural membrane environment, which improves sample stability and facilitates handling.[6,11,24,25]

Before nanosomes deposition onto a SAM, we checked the presence of olfactory receptor cmyc-OR1740 within them using immunological methods. Western blotting analysis was performed using the anti-cmyc antibody. In membrane fraction prepared from yeast cells transformed to express cmyc-OR1740, an immunoreactive band was observed at ∼35 kDa (Figure 2A, lane 1). This shows that cmyc-OR1740 is present in the monomer form, since the calculated molecular weight of its amino acid backbone is ∼36 000. In contrast, no immunoreactivity was detected in control membrane preparations obtained from nontransformed yeast cells (Figure 2A, lane 1).

Figure 2B shows an immunogold transmission electronic micrograph of a membrane vesicle obtained from yeast cells transformed to express cmyc-OR1740. The visualization of several gold particles on the nanosome confirms the presence of cmyc-OR1740. In all experiments, the membrane fraction was additionally sonicated prior to deposition, to yield nanosomes of uniform size of ∼50 nm in diameter.[6]

(26) Jung, L. S. N. K. E.; Stayton, P. S.; Campbell, C. T. *Langmuir* **2000**, *16*, 9421−9432.
(27) Xia, N. S.-P. J. S.; Zareie, M. H.; Campbell, C. T.; Castner, D. G. *Langmuir* **2004**, *20*, 3710−3716.
(28) Sprinke, J. L. M.; Schmitt, H. J.; Guder, H. J.; Angermaier, L.; Knoll, W. *J. Chem. Phys.* **1993**, *99*, 7012−7019.

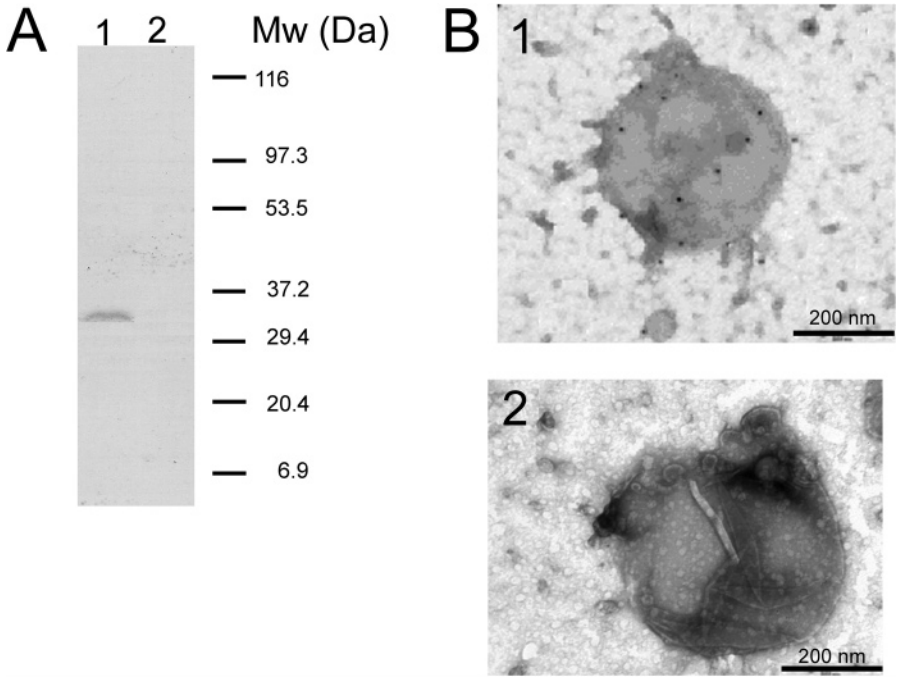

Figure 2. (A) Western blotting analysis of nanosomes obtained from yeast transformed to express cmyc-OR1740 (1), nontransformed yeasts (2) performed using a monoclonal anti-cmyc primary antibody, and HRP-linked anti-mouse IgG as the secondary antibody. (B) A nanosome carrying cmyc-OR1740 (1) is immunolabeled with the primary anti-cmyc antibody and a 10-nm gold-conjugated secondary antibody. Gold grains indicate the presence of the receptor. In control experiments, no gold grains are observed when the primary antibody was omitted (2).

Nanosomes Immobilization. As shown in Figure 3A, two types of procedures were considered to immobilize nanosomes on functionalized surfaces. One involves direct adsorption of nanosomes onto bare SAMs, and the other implies their specific capture via an antibody grafted onto the SAMs. The resulting SPR sensorgrams are given in Figure 3B.

Interestingly, a high level of nonspecific adsorption was observed for all three SAMs. This is probably due to the interaction between hydrophobic alkanethiolate parts of SAMs and the lipidic bilayer of the nanosomes, considering SAMs' low affinity for protein adsorption. These findings suggest that bare SAMs allow cell membranes attachment and thus can possibly be used as a tool for membrane proteins investigations or even whole cell studies. However, this lipid adsorption onto the SAMs can generate a background signal in on-a-chip experiments dealing with membrane proteins. Moreover, these immobilized layers are not stable with time, and receptors are not uniformly orientated on the surface, so that simple adsorption is not a well-adapted method for olfactory receptor assessment. This is especially true for micro- or nanoscale investigations where a tight control of the interaction between biological material and surface is required.

On the other hand, nanosomes were specifically captured via the anti-cmyc antibody. The highest level of SPR signal corresponding to captured receptor (Table 1, column 4), and the highest receptor amount relative to grafted antibody (Table 1, column 5) was obtained for SAM3. This markedly high binding capacity of SAM3 can arise from partially nonspecific adsorption of nanosomes onto unsaturated underlayers. To check this, we deposited nanosomes containing another olfactory receptor, I7, without cmyc tag, and thus not recognized by the anti-cmyc antibody, onto SAM3 modified by neutravidin and anti-cmyc antibody. Comparing the SPR response levels for cmyc-OR1740 nanosome deposition to those for I7 nanosome deposition, it appeared that only ~17% of OR1740 nanosome immobilization could be assigned to specific capture (Figure 3B, SAM3). In contrast, SAM1 and SAM2 modified with neutravidin and anti-cmyc antibody displayed no trend to immobilize nanosomes containing I7 receptor. Consequently, it appears that contrary to SAM1 and SAM2, SAM3 is not well adapted for specific grafting of membrane proteins, but can only and valuably be used for adsorption purposes.

Furthermore, in the case of the capturing procedure, the nanosomes are stably immobilized on the sensor chips. Moreover, they can be stripped from the antibody by several pulses of 10 mM glycine buffer, pH 2.2, which is a standard practice for breaking antibody−antigen bonds. Indeed, three regenerations in a row yielded successive SPR levels for nanosome immobilization with a standard deviation of 4 RU for the four measurements. Thus, it is easy to regenerate the surface and to allow sensor chip reutilization.

We further compared the olfactory receptor surface amount onto SAM1 and SAM2 by performing either capturing or adsorption procedures, through the use of a doubly tagged receptor, cmyc-OR1740-HA. After the receptor capture via its N-terminal cmyc tag, its surface concentration was followed by injecting an anti-HA antibody to quantify C-terminal HA tags. This presupposes that the receptors are randomly oriented in the nanosomes. The SPR signals were compared to those obtained for receptor adsorption obtained onto the bare SAMs, to assess the relative receptor surface concentrations. Interestingly, we found that capturing through an antibody increased surface receptor concentration only by a factor from 9 to 12%, for both SAMs. Similar results were obtained when the receptor surface concentration was investigated using an anti-cmyc antibody after receptor

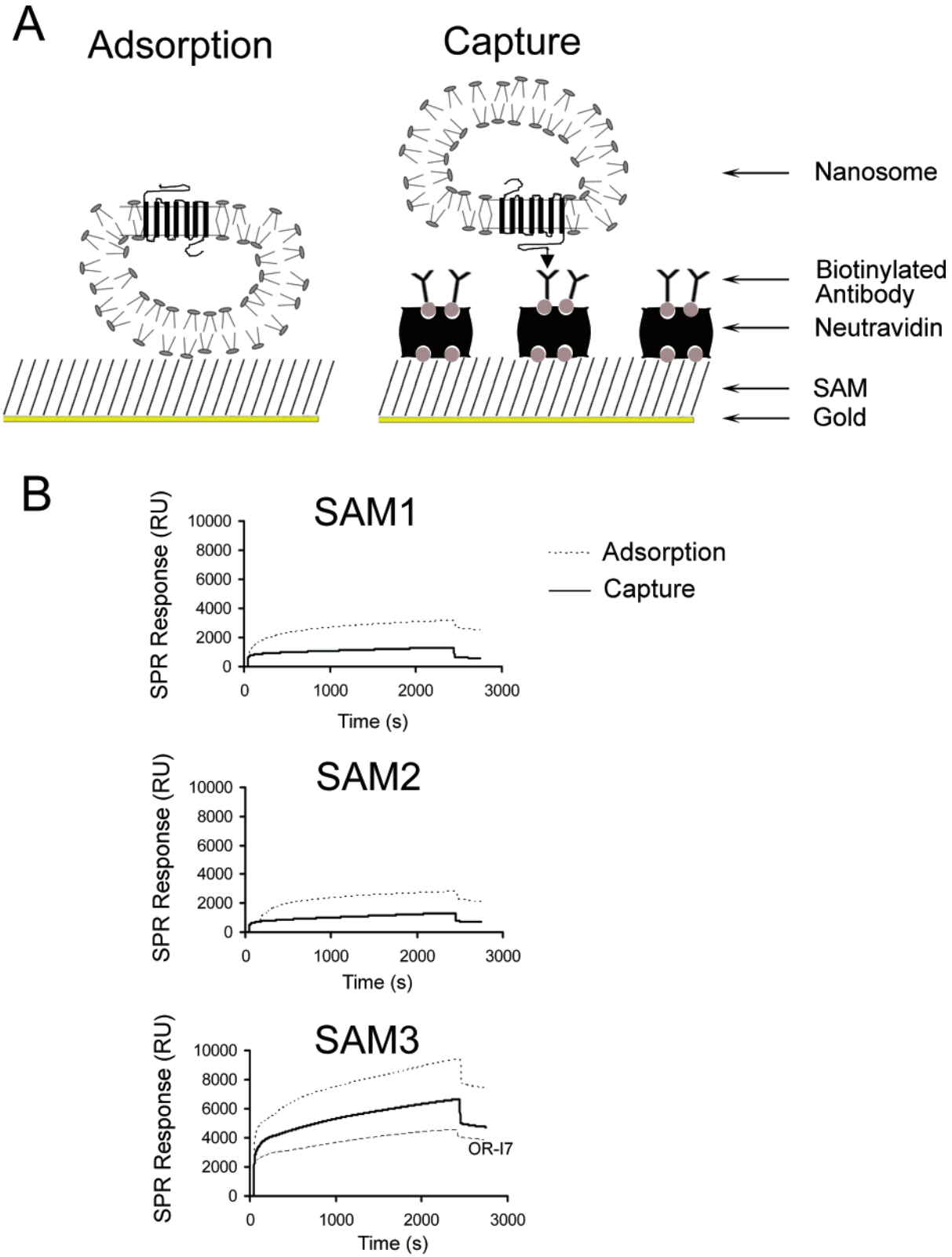

Figure 3. (A) Schematic views of the two modes of nanosome immobilization: nonspecific "adsorption" onto SAM and "capture" by grafting via a specific antibody. (B) SPR sensorgrams showing the response from adsorbed and captured nanosomes carrying cmyc-OR1740 receptor onto the surfaces functionalized by SAMs. The response from nanosomes carrying OR-I7 deposited on SAM3 is also displayed in comparison to cmyc-OR1740.

capturing via HA tag (data not shown). Previously, we had estimated by an ELISA-type test that $\sim 1.44 \times 10^5$ receptors were expressed per yeast cell.[5] This suggests that one nanosome of 50-nm diameter can contain up to 10 olfactory receptors. Thus, the relatively low difference in receptor surface concentration achieved by capture versus adsorption is probably a consequence of the somehow relatively high density of the receptors in the nanosomes.

So, what are indeed the decisive practical advantages of the capturing strategy that makes it better suited for the preparation of membrane receptor chips? (1) Capture increases receptor surface concentration, which is particularly important when the protein of interest is present in a low amount in membrane fraction. (2) It ensures a uniform orientation of immobilized receptor. (3) Only capturing yields a stability of the nanosome layer lasting several days. (4) Finally, the capturing procedure allows regeneration of the sensor chips.

Functional Tests. To assess the functional integrity of immobilized OR1740 carried by nanosomes, its interactions with an odorant were tested. As we demonstrated previously,[6] the expected SPR response subsequent to the interaction of the olfactory receptor with its odorant ligand arises from the activation of the heterotrimeric G protein anchored to the nanosome membrane bilayer. In the presence of GTP (or its analogous GTPγS), which binds to the $G_{\alpha olf}$ subunit, this results in the mobilization of the $G_{\alpha olf}$ subunit, which is easily measured by a significant and reproducible negative variation of SPR signal, indicating the dissociation and departure of a molecular species. Indeed, surface plasmons are sensitive to changes in the optical architecture near the interface, and the SPR signal is a measure of mass concentration at the sensor chip surface.[29] A similar approach has recently been reported with rhodopsin as the GPCR and transducin as the G_α subunit[30] and had indeed been previously validated as a tool for evaluating rhodopsin activation in ref 31. This typical negative SPR signal thus constitutes the signature of the receptor's functionality.

For this study helional, the preferential ligand of OR1740, was used at a concentration of 5 μM. This had induced a maximal SPR shift upon assessment of cmyc-OR1740 function in nanosomes nonspecifically immobilized onto a commercial L1 sensor chip, while other irrelevant odorants failed to induce quantitative responses.[6] Various immobilization conditions were compared. First, we found that even cmyc-OR1740 adsorbed onto bare SAM1−3 responded to helional. Second, no SPR response was observed when nanosomes bearing ORI7 were stimulated with helional, which underlines the response specificity, helional being no ligand for ORI7.

Third, comparing the functional responses of cmyc-OR1740 captured via an anti-cmyc antibody grafted onto SAM1−3, a functional response was observed only with SAM3. The absence of response with SAM1−2 could arise either from a lower surface density of captured cmyc-OR1740 or from the inaccessibility of the odorant binding site in immobilized receptors. Thus, in a fourth set of experiments, helional was applied onto cmyc-OR1740-HA, captured either via cmyc or HA tag onto SAM1−2. Experiments were reproduced 7−9 times for N-terminal capturing via cmyc on each SAM and 2−3 times for octanal control. For C-terminal capturing via HA, three individual experiments were performed on each SAM with each odorant. Strikingly, functional responses were observed only from receptors immobilized via their C-terminal HA tag, which strongly suggests that failure to respond to the odorant originates from steric hindrances to odorant binding due to immobilization of the N-terminus of the receptor. In addition, this would imply that, in the case of cmyc-OR1740 captured via the cmyc antibody on SAM3 (third test), the response only arises from those receptors not bound through the anti-cmyc antibody but plainly adsorbed onto functionalized SAM3.

Finally, we compared the intensities of SPR responses to helional stimulation of cmyc-OR1740-HA immobilized by adsorption or capturing of the nanosomes via the HA tag on SAM1−2. A representative curve from three individual experiments is shown for each SAM in Figure 4. The functional response is increased up to 50% for specific capturing relative to adsorption.

Taken together, these findings show that nanosomes grafting via an antibody specific to the tagged receptor improves the sensor sensitivity. A specific immobilization indeed allows concentrating membrane receptors on the biofunctionalized solid support, thus constituting an in situ selection of these receptors. Furthermore, the results demonstrate that receptor orientation on the surface constitutes a primary requirement to allow functional tests. Katada et al.[32] have reported that N- and C-terminal domains are key elements in the functional expression and signal transducing activity of an olfactory receptor. Their results suggested that the C-terminal portion is involved in receptor interaction with G-protein. Here, we observe that the addition of a C-terminal HA tag used to capture the receptor does not prevent this interaction. In contrast, receptor immobilization by its N-terminal cmyc tag impairs odorant response activity. The N-terminal domain of olfactory receptors is assumed to target these proteins to the secretory pathway.[32] Since cmyc-OR1740 was previously shown to be fully active in living cells,[5,14,33] and in nanosomes nonspecifically immobilized onto a sensor chip,[6] it appears that full flexibility of the receptor N-terminal domain is crucial to allow the proper receptor conformational changes that occur upon receptor−odorant interaction.

Microcontact Printing. We propose strategies for patterning nanosomes onto a solid gold surface by microcontact printing of SAM1−3 (Figure 5A). This can be performed using both BATs and PEGATs, since both react rapidly with gold.[19,34,35] For SAM1, after patterning BATs, the remaining free gold areas were blocked with PEGATs in order to avoid nonspecific adsorption of proteins between patterns. For SAM2, biotin groups were patterned by microcontact printing of EZ-link-Amine-PEO3-Biotin over a previously activated MHDA surface, while blocking of the remaining acid areas was achieved using AEE to reduce nonspecific adsorption. Finally, SAM3 mixed solution cannot be by itself used as an ink for patterning surfaces because cografting of MHDA and biotinyl-PE on the surfaces cannot be performed in a single step. In consequence, SAM3 patterns have to be realized by first patterning a PEGAT blocking molecule on a gold surface and then immersing the surface in MHDA/biotinyl-PE mixed solution. A final immersion of patterned gold surfaces with SAM1−2 in streptavidin−Texas red solution was performed to demonstrate how efficiently the structuration is controlled (Figure 5A).

(29) Pattnaik, P. *Appl. Biochem. Biotechnol.* **2005**, *126*, 79−92.
(30) Komolov, K. E.; Senin, II;, Philippov, P. P.; Koch, K. W. *Anal. Chem.* **2006**, *78*, 1228−1234.
(31) Bieri, C.; Ernst, O. P.; Heyse, S.; Hofmann, K. P.; Vogel, H. *Nat. Biotechnol.* **1999**, *17*, 1105−1108.
(32) Katada, S.; Tanaka, M.; Touhara, K. *J. Neurochem.* **2004**, *90*, 1453−1463.
(33) Wetzel, C. H.; Oles, M.; Wellerdieck, C.; Kuczkowiak, M.; Gisselmann, G.; Hatt, H. *J. Neurosci.* **1999**, *19*, 7426−7433.
(34) Yan, L. Z. X.-M.; Whitesides, G. M. *J. Am. Chem. Soc.* **1998**, *120*, 6179−6180.
(35) Lenz, P. A.-F. C. M.; Boxer, S. G. *Langmuir* **2004**, *20*, 11092−11099.

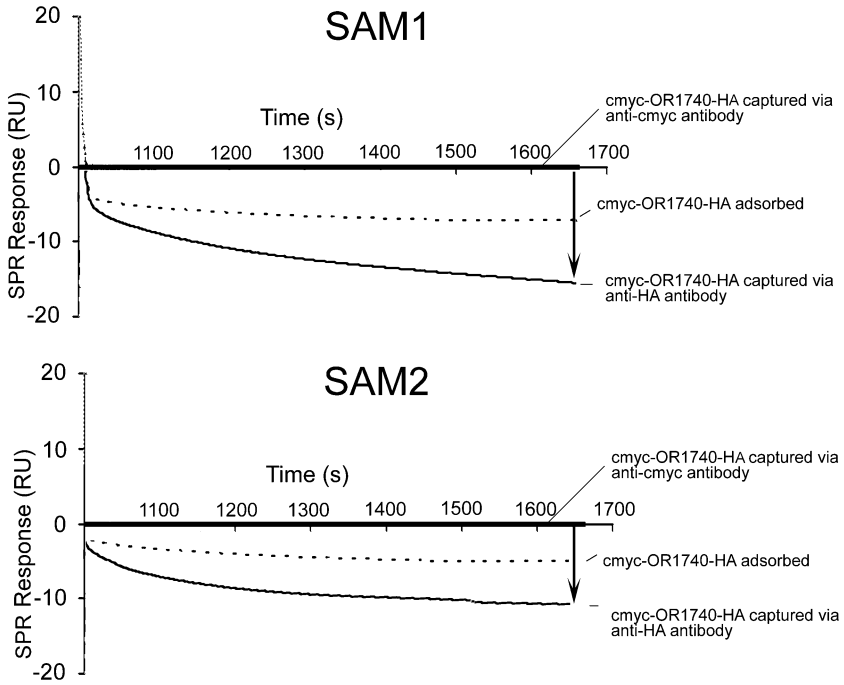

Figure 4. Differential SPR sensorgrams showing signal modifications observed when helional and GTPγS are simultaneously injected over immobilized nanosomes. Signal responses are normalized to the corresponding controls obtained by replacing odorant with water. No specific response is obtained starting from nanosomes with ORI7, for which helional is not a ligand (not shown). The intensity of the specific response of cmyc-OR1740-HA is enhanced in the case of captured nanosomes, via an antibody to the C-terminal tag (arrows) compared to adsorption. There is no functional response when cmyc-OR1740-HA is immobilized via an antibody to the N-terminal tag.

Although the same stamps were used for both SAM1 and 2, the spots look different. Inks used for SAM1 resulted in a diffusion, which led to the inhomogeneous rings on the borders of the spots, quite different from the pattern observed for SAM2. It is probably a matter of differing ink viscosity and surface tension, so that when the stamp is relieved from the surface after microcontact, the ink may flow from the sides of the protruding posts and leave this ringlike structure combined with the spots pattern. The experiment was attempted with SAM3 but gave rise to a strong background staining, confirming nonspecific adsorption of neutravidin observed by SPR.

Nanosomes patterning can then be achieved by successive immersion of gold surfaces patterned with SAMs in neutravidin, biotinylated antibody solution, and then a suspension of freshly sonicated nanosomes. Figure 5B shows AFM visualization of such grafted nanosomes (cmyc-OR1740 on anti-cmyc antibody) on SAM1. While nanosomes in suspension have diameters of ~50 nm, their diameter size ranges from 50 to 1000 nm at the surface (Figure 5B). This suggests that immobilized nanosomes have a tendency to fuse into larger ones but, however, not into a continuous membrane bilayer.

CONCLUSIONS

In this study, olfactory receptors carried by nanosomes were successfully immobilized onto biosensor surfaces functionalized by mixed self-assembled monolayers and biotin/neutravidin. Such systems can detect a receptor-specific odorant with label-free SPR measurements, indicating that receptor functionality is preserved. Moreover, the immobilization strategies used are well adapted for micro- and nanosensor formats. Specific immobilization by capturing the receptors via an antibody yields a uniform orientation of the receptor onto the surface, and at least for OR1740, grafting via a C-terminal tag is adequate for preserving the receptor activity. In addition, a limited enrichment in membrane receptors on the biofunctionalized solid support is obtained as a result of the in situ selection of the receptor.

The SPR functional test showed that SAM3 is not well suited for olfactory biosensor elaboration, regarding a relatively low level of neutravidin binding and a high level of nonspecific adsorption of nanosomes. Concerning the functional test, SAM1 and 2 were found to score similarly. However SAM1 exhibits definite advantages relative to SAM2 for micro- and nanosensor applications: (i) SAM1 can be microcontact-printed onto gold through a single-step procedure, while two steps are required for SAM2. (ii) SAM1 has fewer biotinyl groups than SAM2 but shows the same efficiency for neutravidin binding as SAM2. (iii) AFM imaging of nanosomes deposited onto a microcontact printed SAM2 surface shows some nonspecific nanosome immobilization onto the surfaces blocked with AEE, whereas almost no nonspecific binding of nanosomes is observed with SAM1 where PEGATs are used as blocking agents.

We consider that our findings could be extended for studying other GPCRs, present in a low amount in membrane fractions. Our approach should offer substantial advantages, such as providing a biosensor format for studying receptor−agonist and antagonist interactions, or the influence of membrane lipidic composition on receptor activity. Furthermore, this overall strategy of nanosomes grafting can potentially be adapted for mammalian and microbial cell immobilization, and some new functional assay could be developed for investigating membrane receptor interactions with cellular downstream signaling proteins.

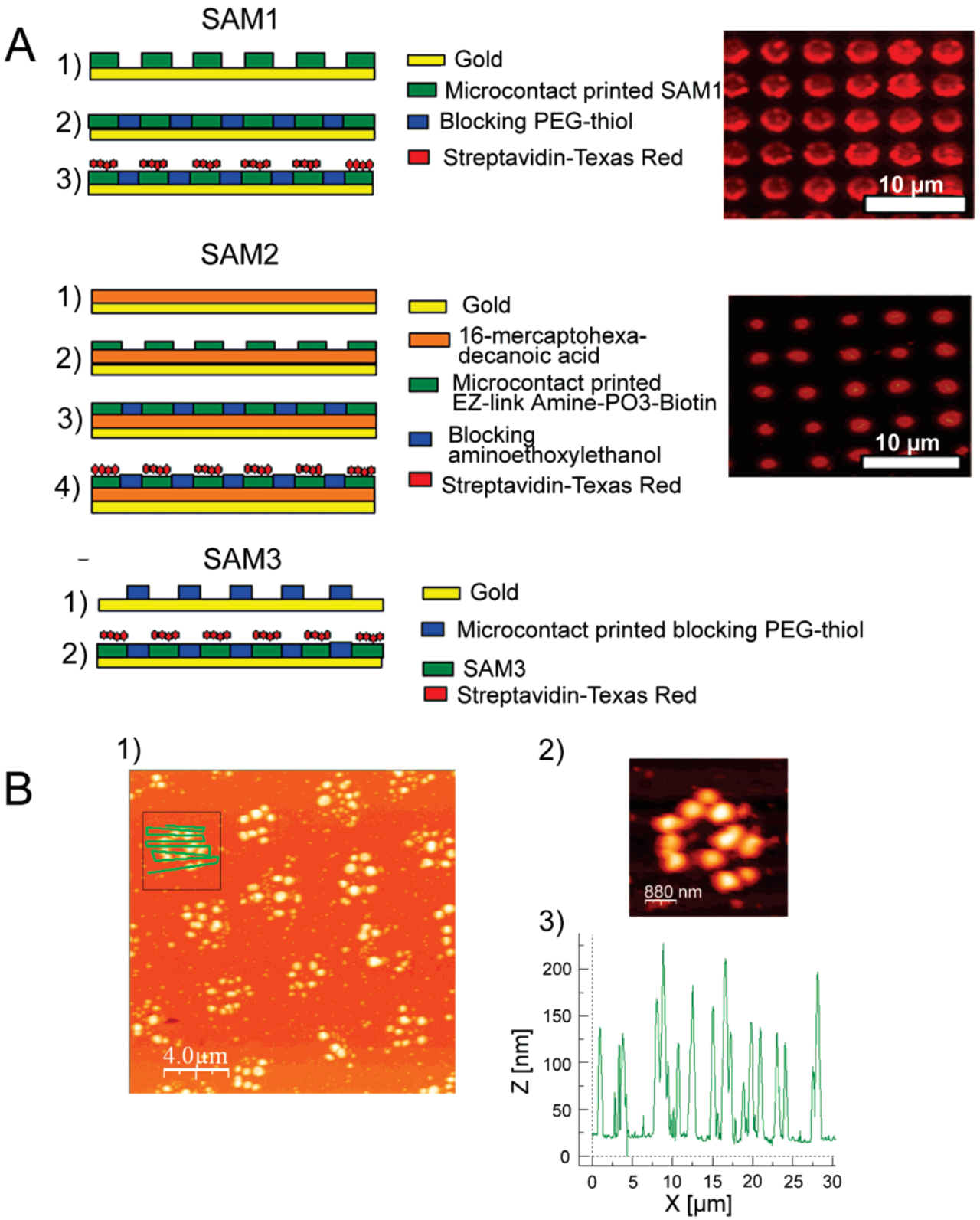

Figure 5. (A) Schematic representation of the procedure used to immobilize SAM1−3 onto the gold surfaces by microcontact printing. The patterning of surfaces is confirmed by fluorescent images of streptavidin labeled with a fluorescent dye, attached onto SAM biotinyl groups. (B) (1) An AFM image shows features at the nanometric scale on the surface functionalized with SAM1 after nanosome deposition. (2) High-resolution topography of the area outlined by the box in (1). (3) A horizontal cross section along the developed green line from (1) reveals the thickness of the immobilized features from (2).

ABBREVIATIONS

AEE, aminoethoxyethanol; BAT, biotin-terminated alkyl thiol; biotinyl-PE, 1,2-dioleoyl-*sn*-glycero-3-phosphoethanolamine-*N*-(biotinyl) sodium salt; BSA, bovine serum albumin; DIPEA, *N*,*N*-diisopropylethylamine; DMSO, dimethyl sulfoxide; EDC, 1-ethyl-3-(dimethylamino)propylcarbodiimidehydrochloride; EZ-Link Amine-

PEO3-Biotin, (+)-biotinyl-3,6,9-trioxaundecamine; GPCR, G protein coupled receptor; MHDA, 16-mercaptohexadecanoic acid; PEGAT, PEG-terminated alkylthiol PFP, pentafluorophenol; PBS, phosphate buffer saline; SPR, surface plasmon resonance.

ACKNOWLEDGMENT

We thank Drs J. Bausells and G. Villanueva (CNM, Barcelona) for providing the DRIE molds for micro-contact printing studies, and Prof. F. Albericio and E. Prats-Alfonso (IRBB, Barcelona) for the gift of BATs and Dr C. Lopez-Iglesias and G. Martínez Ruíz for their kind help on the immunogold studies. We wish to warmly thank Dr Monique Caillol (NOPA-RCC, Jouy en Josas) for her critical reading of the manuscript. This work was financially supported by the PICASSO program (HF2004-0055) funded by EGIDE and the SPOT-NOSED project (IST-38899) funded by the Future and Emerging Technologies arm of the IST program FET-Open scheme (European Community).

Received for review September 20, 2006. Accepted February 20, 2007.

AC061774M